Suppression of the observation of Stark ladders in optical measurements on superlattices by excitonic effects

A. M. Fox
Department of Physics, University of Oxford, Clarendon Laboratory, Parks Road, Oxford OX1 3PU, United Kingdom

D. A. B. Miller, J. E. Cunningham, and W. Y. Jan
AT&T Bell Laboratories, Crawfords Corner Road, Holmdel, New Jersey 07733

C. Y. P. Chao and S. L. Chuang
Department of Electrical and Computer Engineering, University of Illinois, 1406 West Green Street, Urbana, Illinois 61801
(Received 4 August 1992)

We investigate experimentally and theoretically how excitonic effects influence the optical properties of semiconductor superlattices in the Stark-ladder regime. Excitonic effects are particularly important when the superlattice miniband width is comparable to the exciton binding energy. In order to observe a Stark ladder it is necessary that either the electron or hole wave function (or both) be at least partially delocalized. In an optical experiment the delocalization of the wave functions is affected by the electron-hole Coulomb interaction. Excitonic effects can therefore prevent the observation of the Stark ladder if the Coulomb interaction is strong enough to localize the wave functions completely. We have studied three $GaAs/Al_{0.3}Ga_{0.7}As$ superlattices, with calculated conduction-band miniband widths ΔE of 6, 11, and 23 meV. Experimentally, we observe a heavy-hole Stark-ladder fan diagram in the sample with the 23-meV miniband width, which indicates an electron wave-function delocalization over several superlattice periods. However, in the other two samples in which ΔE is comparable to the exciton binding energy, we do not observe a fan diagram, which indicates much stronger wave-function localization. Instead, we observe an anticrossing at a field strength of $\sim 5\ \mathrm{kV\,cm^{-1}}$. In these conditions, the multiwell structure behaves more like many repeated pairs of coupled double wells rather than a superlattice. We interpret the observed anticrossings at $\sim 5\ \mathrm{kV\,cm^{-1}}$ in the samples with the smaller miniband widths as an excitonic degeneracy similar to that observed previously at higher fields [A.M. Fox *et al.*, Phys. Rev. B **44**, 6231 (1991)]. We have been able to explain this behavior using both a variational exciton model based on three coupled quantum wells and a full Green's-function solution for the excitons assuming a double-quantum-well structure.

I. INTRODUCTION

Quantum theory predicts that when an electric field is applied to a periodic structure, there should exist a ladder of equally spaced energy levels whose separation depends linearly on both the electric-field strength and the periodicity.[1] This ladder of levels is referred to as the Stark ladder. The Stark ladder is the frequency space equivalent of Bloch oscillations, the phenomenon by which the particle is predicted to oscillate in space at a frequency equal to the Stark-ladder splitting divided by Planck's constant. Although the Stark ladder and Bloch oscillations are completely general properties of any periodic structure in an electric field, they are in fact very hard to detect experimentally. The reason for this is that the oscillation period is usually much longer than the scattering times of the material.

The proposal of Esaki and Tsu in 1970 to explore the properties of artificially periodic superlattice structures made by the epitaxial growth of semiconductors opened new degrees of freedom to the problem.[2] Even in their initial paper the possibility of the observation of Bloch oscillations was considered: the prospect of making the superlattices with periods long enough that the Bloch oscillation time would be less than the scattering time made it realistic to expect to observe the Stark-ladder states. However, the first experimental results on periodic multiple-quantum-well structures in an electric field showed no evidence either for the Stark ladder or Bloch oscillations,[3–5] and the results could be explained just by considering the properties of single isolated quantum wells.[6,7]

Insight into the question came in 1988, when Bleuse, Bastard, and Voisin considered theoretically the localizing effect of the electric field on the electron and hole superlattice wave functions.[8] This was followed by the experimental observation of the Stark ladder later in the same year by Mendez, Agullo-Rueda, and Hong.[9] The experimental verification came from the optical spectra of a $GaAs/Al_xGa_{1-x}As$ superlattice. At an intermediate range of electric field strengths, they observed a series of satellite peaks associated with the first heavy- and light-hole optical transitions. The transition energies of these satellite peaks ($\hbar\omega$) were found to have a very simple

linear dependence on the field strength (F_z) and the superlattice periodicity d:

$$\hbar\omega(F_z) = \hbar\omega_0(F_z) + \nu eF_z d\,, \tag{1}$$

where $\hbar\omega_0(F_z)$ is the Stark-shifted energy of the fundamental transition, $\nu = 0, \pm1, \pm2, \ldots$, etc., and e is the electronic charge. The satellite peaks originated from transitions involving a *single* heavy-hole level and *several* levels from the electron Stark ladder, as sketched in Fig. 1, where the transitions corresponding to $\nu = -1$, 0, and -1 are indicated. In principle these transitions were always present in the early experimental work cited above, but in practice only the transition with $\nu = 0$ was being observed. The difference between the work of Ref. 9 and the previous studies was in the extent of wave-function delocalization in the conduction band with the field applied. At the intermediate fields, the electron wave functions associated with each Stark-ladder level were partially delocalized, with each wave function being peaked in a particular quantum well but with substantial side lobes extending into a few quantum wells on either side of the main peak (see Fig. 1). The hole wave functions, on the other hand, were localized in just one particular quantum well. This meant that there was a significant overlap integral between a hole state localized in one quantum well and an electron state peaked in a different quantum well, resulting in a detectable optical transition. The energy shift from the fundamental transition was simply due to the energy difference of ($eF_z d$) between the electron Stark-ladder levels. Thus we see that the successful experimental observation of the Stark ladder requires at least partial delocalization of either the electron wave function or the hole wave function (or both) at finite fields.

In this work we consider both experimentally and theoretically how excitonic effects can modify the optical spectra of semiconductor superlattices in the Stark-ladder regime. Previous studies of excitonic effects in Stark ladders have been entirely theoretical.[10–16] In principle, excitonic effects are always important in optical measurements on semiconductors, because electrons and holes are always created simultaneously. Indeed, the experimental work of Mendez, Agullo-Rueda, and Hong demonstrating the existence of the Stark ladder was in fact made by measuring the field dependence of the exciton states rather than single-particle states.[9] In practice, however, excitonic effects are usually considered as secondary in Stark-ladder studies on superlattices. One way of rationalizing this is that the samples studied tend to have superlattice miniband widths significantly larger than the exciton binding energy. Hence we might expect that the excitonic effects are then not strong enough to suppress the superlattice effects. Here we consider the case of superlattices in which the miniband width and the exciton binding energy are comparable. Our principal conclusion is that excitonic effects can lead to a situation where no Stark-ladder fan diagram is observed in optical experiments in superlattices where one would otherwise have expected to be able to observe Stark-ladder effects. This is a consequence of the fact that delocalized wave functions are required at finite fields in order to observe the Stark ladder in an optical experiment, and the excitonic effects can substantially reduce the delocalization of the electronic wave functions. This leads to a physical situation similar to that reported in the early (and much subsequent) work on multiple-quantum-well samples in an electric field,[3–5,7] where no Stark-ladder effects were observed due to the strong degree of localization of both the electron and hole wave functions. We presume that in these samples the Stark-ladder states exist when the field is applied, but that we have no way of verifying this in an optical experimental because of the negligible overlap between electron and hole states in different quantum wells.

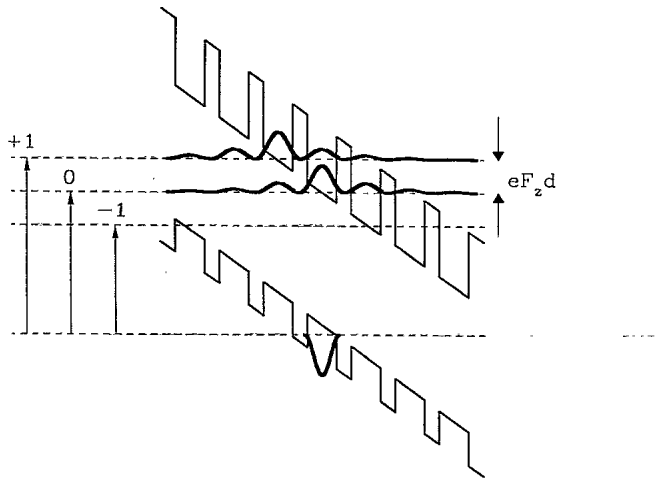

FIG. 1. Schematic band diagram of a superlattice with period d in an electric field of strength F_z. The Stark-ladder transitions with $\nu = +1$, 0, and -1 from a particular heavy-hole state are indicated. The oscillator strength of the transition depends on the electron-hole overlap. The wave functions shown are the probability densities for the single particle wave functions, not the excitonic wave functions.

The principal experimental result that leads us to our conclusions is that we find that, in samples where the exciton binding energies are comparable to or larger than the miniband widths, we are unable to observe the characteristic Stark ladder, even when we can clearly see that the electron and hole wave functions in adjacent wells have strong overlap. Instead we observe a very clear excitonic anticrossing at a field strength of about 5 $\mathrm{kV\,cm^{-1}}$. We have been able to explain this anticrossing behavior by assuming that the adjacent wells from within the superlattice are behaving like many repeated pairs of coupled double wells independent of the remaining wells of the superlattice. It is then a relatively straightforward exercise to calculate the properties of the superlattice excitons using a coupled-well exciton model such as the one we developed previously.[17,18] This amounts to a considerable simplification compared to the full superlattice exciton Stark-ladder theories considered so far in the literature.[10–16]

The paper is organized as follows. In Sec. II we explain the basic ideas underlying our argument. In Sec. III we present and discuss our experimental results. In Sec. IV

we describe the coupled-well exciton calculations we have performed to model the experimental results. Finally, in Sec. V we draw our conclusions.

II. PRELIMINARY CONSIDERATIONS

A superlattice may be considered as a periodic sequence of quantum wells connected together through "thin" separating barriers. When the barriers separating the quantum wells are "thick," the properties of the superlattice are essentially the same as those of the isolated quantum wells, and therefore this class of superlattice is usually called a "multiple quantum well" rather than a "superlattice." This is tantamount to saying that the miniband width ΔE of these "thick" barrier superlattices is negligibly small. An obvious question arises as to what is the criterion that determines whether the barriers of a particular sample are "thick" or "thin." The answer to this question depends on the type of measurement that is being made. The crux of our argument is that the criterion is different depending on whether the type of measurement is optical or electrical. This is because in an optical experiment electrons and holes are created simultaneously, and it is necessary to consider the Coulomb interaction between them. We argue below that the criterion which determines whether a particular sample behaves like a "superlattice" or a "multiple quantum well" for the purposes of an optical experiment depends on the relative magnitude of the miniband widths and the exciton binding energy, and that the Stark-ladder spectra are a sensitive experimental technique which can show the difference between the two classes of behavior.

The effects of the electron-hole Coulomb interaction on the Stark-ladder spectra are simpler to understand if we restrict our discussion to the case of heavy-hole excitons only. This is because the heavy-hole superlattice miniband width is almost negligible, and so the heavy holes are always effectively localized in just one quantum well in the conditions that apply to our samples; for all practical purposes, we may use the heavy-hole wave functions of a single, isolated quantum well. This means that we need only consider the effect of the Coulomb interaction on the delocalization of the electron wave functions. The case of light-hole excitons is complicated by the fact that the light-hole miniband width is typically comparable to the electron miniband width, and thus one needs to consider the effects in both the conduction and valence band. In the argument that follows, we will consider only heavy-hole excitons; later in the paper we will discuss the validity of our argument in the case of light-hole excitons.

When electrons and holes are both present in a superlattice (as is the case for optical measurements), the superlattice states are modified by the electron-hole Coulomb interaction. The exciton may be described by a wave function of the form

$$\Psi(\mathbf{r}_e,\mathbf{r}_h)=\psi_{\mathrm{c.m.}}(X,Y)\,\psi_{\mathrm{rel}}(x,y)\,\psi_e(z_e)\,\psi_h(z_h)\ , \qquad (2)$$

where the growth direction is taken to be the z axis, and $\mathbf{r}_e$ and $\mathbf{r}_h$ are the electron and hole coordinates. For the x-y plane motion, we have made the usual distinction between the center-of-mass motion with wave function $\psi_{\mathrm{c.m.}}(X,Y)$ and the relative motion with wave function $\psi_{\mathrm{rel}}(x,y)$. For the z-direction motion we consider separately the electron and hole parts of the wave function, $\psi_e(z_e)$ and $\psi_h(z_h)$, respectively. In the case of a heavy-hole exciton, $\psi_h(z_h)$ will usually be localized in one quantum well at all fields, whereas $\psi_e(z_e)$ will spread over a number of wells at low fields and gradually become more localized as the field is increased. Figure 1 illustrates the probability densities for typical wave functions $\psi_e(z_e)$ and $\psi_h(z_h)$ at an intermediate field strength where the electron wave functions spread out over several wells. It is the spread of $\psi_e(z_e)$ at finite fields which determines how many Stark-ladder transitions are observed.[9,19] This spread of $\psi_e(z_e)$ can be characterized by an effective width, which is equivalent to an effective z-direction exciton radius a_z. This approach is similar to that of Pereira *et al.*, who considered the problem of superlattice excitons by treating the superlattice as an anisotropic medium with different effective masses along the x-y and z directions.[20] The key point of our argument is to realize that a_z is *not* the same as the effective width of the single-particle electron state calculated without taking excitonic effects into account: the presence of the localized hole reduces the spread of the electron wave function. This will have consequences for the number of Stark-ladder transitions observed, and can lead to a situation where only the $\nu=0$ transition is observed. In these conditions we would say that the observation of the Stark ladder has been suppressed by the excitonic effects.

The degree to which the excitonic effects alter the spread of the electron wave function in a heavy-hole exciton is determined by the relative magnitude of the electron-hole Coulomb interaction and the delocalization energy of the superlattice. The Coulomb interaction tries to reduce the effective width of $\psi_e(z_e)$ in order to minimize the potential energy, but there is a price in kinetic energy to be paid to localize the electron. In general the kinetic energy of the single-particle ground state of a superlattice is lower than that of the corresponding isolated quantum well by approximately $\Delta E/2$, where ΔE is the miniband width.[21] This reduction in kinetic energy is a consequence of the delocalization of the wave functions which occurs in the superlattice. Thus it becomes clear that $\Delta E/2$ has to be compared to the quantum-well exciton binding energy E_x to determine the spread of $\psi_e(z_e)$ in the superlattice exciton. In the case of wide miniband superlattices (i.e., superlattices with "thin" barriers), a_z will approach the exciton radius of the bulk alloy with the same average composition as the superlattice. On the other hand, in a narrow miniband superlattice (i.e., "thick" barrier superlattices) a_z will just be equal to the width of one quantum well. We can thus give a rough general criterion which determines what is meant by a "thin" or "thick" barrier superlattice for the case of an optical experiment. A "thin" barrier superlattice is one which has $\Delta E/2 \gg E_x$, whereas a "thick" barrier superlattice (i.e., a "multiple quantum well") has $\Delta E/2 \ll E_x$. For the case of $GaAs/Al_xGa_{1-x}As$ quantum wells, E_x is typically ~ 9 meV. In Sec. III we present experimental results for three $GaAs/Al_xGa_{1-x}As$ samples with calculated values of $\Delta E/2$ of about 11.5, 5.5, and 3 meV,

respectively, for the electron minibands. These samples have thus allowed us to explore the interesting regime where the miniband and excitonic effects are of similar strength.

Figure 2 sketches some of the electron and heavy-hole wave functions in a superlattice in which the electron states are localized at a finite field. This is the case that applies to the single-particle states in "thick" barrier superlattices, and also to the exciton states in superlattices with intermediate barrier thicknesses where the Coulomb interaction causes the localization. In these conditions, we would expect to observe only the $\nu = 0$ Stark-ladder transition, because this is the only transition which has a substantial electron-hole overlap. However, there is still a vestige of the Stark ladder which occurs around a particular resonant field in the superlattices where the electron wave function has been localized by the Coulomb interaction. This happens because the barriers are still relatively thin (35 Å at most in the case of our samples), and the electrons can still tunnel very easily through the thin barriers. In particular, resonant tunneling can occur when the field aligns different sublevels of adjacent wells. The samples then behave like many repeated pairs of coupled double wells rather than a superlattice. We showed previously that the *excitonic* tunneling resonances of coupled wells occur at slightly different fields from the single-particle resonances.[17,18] Similar behavior has also been discussed by other groups.[22–24] This is a consequence of the fact that the binding energies of the intrawell and interwell excitons differ by about 4 meV.[18] When the field applied is such that the energy drop between wells is equal to this difference in binding energy, then the intrawell and interwell *excitons* will be degenerate, even though the single-particle levels are out of resonance with each other. This situation is sketched schematically in Fig. 2. In these conditions the intrawell and interwell excitons mix together and share their oscillator strength, so that the -1 exciton Stark-ladder transition becomes observable. In our samples, this excitonic resonance occurs around 5 kV cm^{-1}. This anticrossing is in fact just the excitonic counterpart of the fundamental level repulsion which occurs at $F_z = 0$ in a symmetric coupled double-well structure. Experimentally, we observe anticrossings in the excitonic transitions of two of our samples at fields around 5 kV cm^{-1}, which we attribute to this excitonic degeneracy.

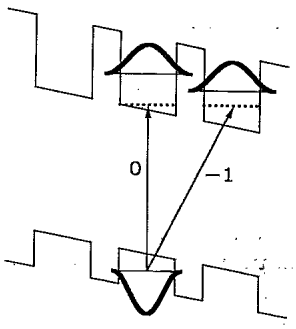

FIG. 2. Schematic band diagram of three quantum wells from within a superlattice with localized electron levels at the resonant field for exciton resonant tunneling (~ 5 kV cm^{-1} in our samples). The dotted lines indicate the exciton energies relative to the single-particle hole level. The intrawell (0) and interwell (-1) excitons are degenerate. The exciton transitions observed in the optical spectra of two of our samples at this resonant field are indicated.

Similar anticrossing effects to those described above have been discussed by Dignam and Sipe in terms of a full superlattice exciton Stark-ladder model.[12] Our situation lies between the long-period and intermediate-period superlattices considered by them. We are describing the exciton energies approximately by Eq. (3.1) of Ref. 12, which applies to the case of long-period superlattices. However, we have enough cross-well coupling to observe the anticrossing of 0 and -1 exciton Stark-ladder states, which is illustrated in Fig. 6 of Ref. 12 for the case of intermediate-period superlattices.

III. EXPERIMENTAL RESULTS AND DISCUSSION

The three GaAs/$Al_{0.3}Ga_{0.7}As$ p-i-n superlattice structures studied have been described in detail in a previous publication.[18] In brief, they were grown on n doped GaAs substrates by molecular-beam epitaxy. The nominal well width was kept constant at 95 Å, but the barrier width L_b varied from 35 to 15 Å. The p and n doping densities were both 5×10^{17} cm^{-3} . The samples were designed with an intrinsic region thickness of ~ 1 μm. X-ray data and detailed analysis of the optical spectra confirmed the design parameters to better than 10% . The design of the samples allowed a systematic variation of the cross-well coupling (determined by L_b), while keeping all other parameters constant as far as possible.

Figures 3, 4, and 5 show the experimental results taken for the three samples close to flat-band conditions at low temperatures. Figures 3(a), 4(a), and 5(a) show the photocurrent spectra in the vicinity of the fundamental band edge as a function of applied voltage. Positive voltage implies forward bias. Figures 3(b), 4(b), and 5(b) show the energies of various transitions resolved in the spectra against field, together with the results of our theoretical calculations described in Sec. IV A. The filled and open circles refer to heavy- and light-hole transitions, respectively. The transition energies are plotted against field strength F_z, which is deduced from the applied voltage $V_{\rm appl}$ according to

$$F_z = \frac{V_{\rm bi} - V_{\rm appl}}{L} . \tag{3}$$

Here L is the intrinsic region thickness, i.e., ~ 1 μm, and $V_{\rm bi}$ is the effective built-in voltage of the diode. The value of $V_{\rm bi}$ varies somewhat from sample to sample due to differing impurity concentrations, which causes a different degree of depletion in the diode. To fit our data, we vary $V_{\rm bi}$ between 1.0 and 1.5 V, depending on the sample, as discussed below.

We show the spectra up to a maximum value of -1.0 V reverse bias. At this voltage the field strength is $\approx$20–25 kV cm^{-1}, and the energy drop between adjacent

wells is greater than the electron or light-hole miniband width for all three samples. Thus at −1.0 V, the electron and hole wave functions are localized in individual wells, and the band-edge spectra are dominated by the heavy- and light-hole exciton transitions as for conventional multiple-quantum-well structures. The linewidth of these exciton transitions increases with decreasing L_b, presumably due to lifetime broadening by enhanced tunneling in the thinner barrier samples. The transition energies of the n=1 heavy- and light-hole exciton lines at larger values of reverse bias (i.e., fields up to ~ 80 kV cm^{-1}) are shown as insets in Figs. 3(b), 4(b), and 5(b). The exciton lines are observed to redshift as appropriate for localized excitons in the quantum confined Stark effect regime.[7] Anticrossings, which are not shown for clarity in Figs. 3(b), 4(b), and 5(b), are observed for all three samples in the field range around 80 kV cm^{-1}. In a previous publication we have shown that this is a coupled-well effect in which the $e1$ level of each quantum well is made degenerate with the $e2$ level of the next

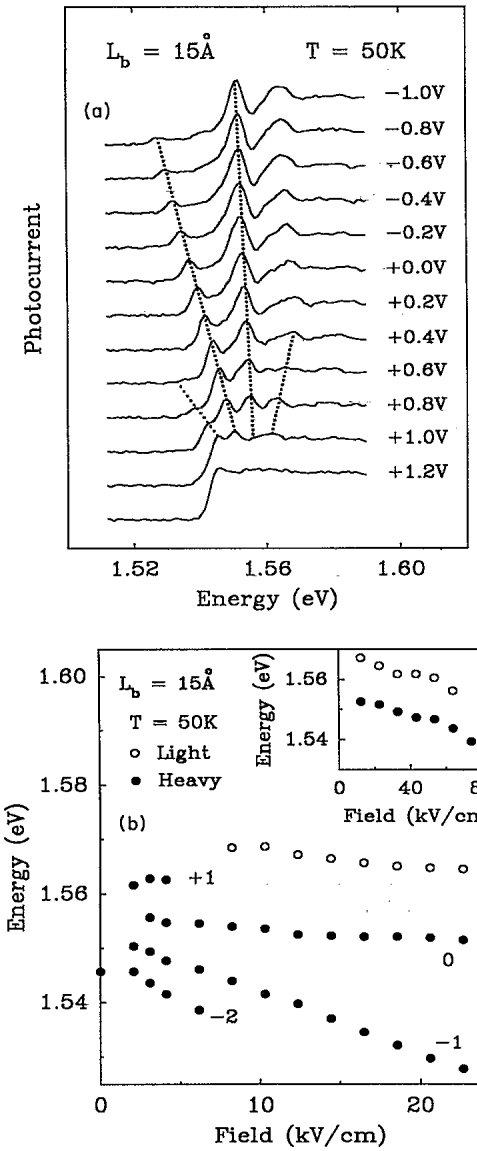

FIG. 3. Experimental results for the GaAs/$Al_{0.3}Ga_{0.7}As$ multiple-quantum-well p-i-n sample with barrier thickness L_b=15 Å at 50 K. (a) Band-edge photocurrent spectra against bias voltage. (b) Exciton transition energies resolved in the photocurrent spectra against field up to 25 kV cm^{-1}. The inset of (b) shows the Stark-shifting n=1 heavy- and light-hole exciton energies up to 80 kV cm^{-1}. The dotted lines plotted over the spectra in (a) are a guide to the eye.

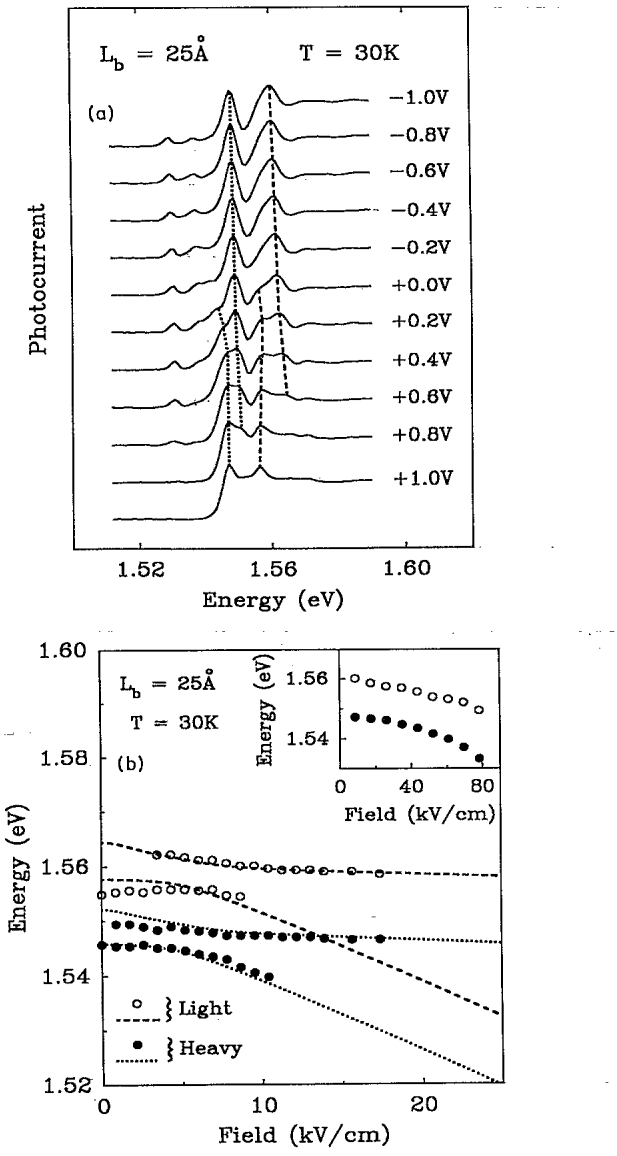

FIG. 4. Experimental and theoretical results for the GaAs/$Al_{0.3}Ga_{0.7}As$ multiple-quantum-well p-i-n sample with barrier thickness L_b=25 Å at 30 K. (a) Band-edge photocurrent spectra against bias voltage. (b) Exciton transition energies resolved in the photocurrent spectra against field up to 25 kV cm^{-1}. The inset in (b) shows the n=1 heavy- and light-hole exciton energies at larger field strengths. In (b) we compare the experimental data with the −1th and 0th Stark-ladder exciton transition energies calculated from our three-well variational exciton model. The dotted and dashed lines over the spectra in (a) are a guide to the eye.

well.[18] This paper is concerned with the behavior of the optical spectra as the applied field is decreased towards flat-band conditions.

We consider first the results for the 15-Å barrier sample (electron miniband width $\Delta E \sim 23$ meV) shown in Fig. 3. We observe a well-defined heavy-hole Stark ladder for fields up to ~ 25 kV cm^{-1}, similar to the results obtained previously by other groups.[9] The point about this sample is that $\Delta E/2$ is greater than the quantum-well exciton binding energy (~ 9 meV), and thus we would not expect the excitonic effects to be particularly important. The family of Stark-ladder transitions is clearest at +0.8 V, where three peaks are resolved in the spectra corresponding to the $\nu = -1$, 0, and +1 heavy-hole Stark-ladder transitions. A shoulder on the low-energy side of the -1 peak is also observed, which we assign to the $\nu = -2$ transition. The fanlike behavior of the state energies as a function of field predicted by Eq. (1) is evident from the dotted lines plotted over the data as a guide to the eye in Fig. 3(a), and also from inspection of Fig. 3(b).

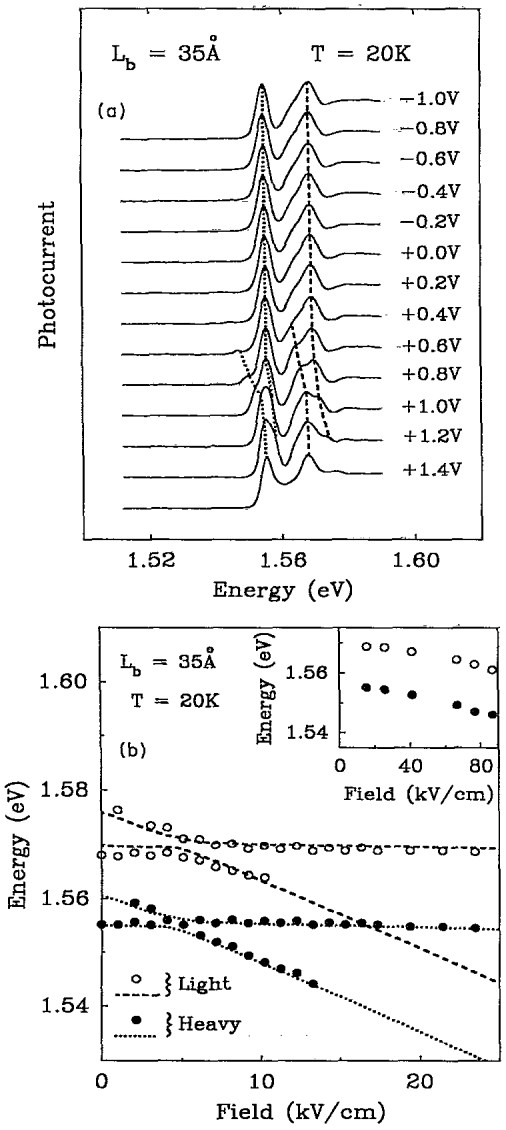

FIG. 5. Experimental and theoretical results for the GaAs/$Al_{0.3}Ga_{0.7}As$ multiple-quantum-well p-i-n sample with barrier thickness L_b=35 Å at 20 K. (a) Band-edge photocurrent spectra against bias voltage. (b) Exciton transition energies resolved in the photocurrent spectra against field. The inset in (b) shows the n=1 heavy- and light-hole exciton energies at larger field strengths. In (b) we compare the experimental data with the -1th and 0th Stark-ladder exciton transition energies calculated from our three-well variational *exciton* model. The dotted and dashed lines over the spectra in (a) are a guide to the eye.

In Fig. 3(b) we converted between applied voltage and field using Eq. (3) with a value of 1.2 V for V_{bi}. An accurate conversion between the known applied voltage and the inferred internal field is essential for a quantitative analysis of the results, and this depends critically on the value of V_{bi} chosen. We arrived at the value of 1.2 V for V_{bi} from analysis of the experimental data. The photocurrent spectrum at $V_{appl} = +1.2$ V forward bias shown in Fig. 3(a) has no easily resolved exciton lines, and the absorption edge is significantly downshifted compared to the 0th Stark-ladder transition. We interpret this as an indication of miniband formation, which suggests that at +1.2 V we are very close to flat-band conditions. Additional evidence to support this value for V_{bi} is obtained from the magnitude of the photocurrent collected. This depends on the quantum efficiency of the diode, which was found to drop off very rapidly for $V_{appl} > +1.2$ V. This drop in quantum efficiency is to be expected near $F_z = 0$.[25] Thus we have two experimental indications to support the value of ≈ 1.2 V chosen for V_{bi}.

We now turn to the results for the 25-Å sample (miniband width 11 meV) and the 35-Å sample (miniband width 6 meV) shown in Figs. 4 and 5, respectively. It is immediately obvious that the spectra are qualitatively different from that obtained for the 15-Å barrier sample. Rather than observing the characteristic Stark-ladder fan diagram, we observe an anticrossing in both the light- and heavy-hole exciton transitions.[26] This is more apparent from the lines plotted as a guide to the eye in Figs. 4(a) and 5(a), and from inspection of the field dependence of the exciton transitions shown in Figs. 4(b) and 5(b). As for the 15-Å sample, we converted applied voltages into fields by assuming values for V_{bi}. The values used for V_{bi} were 1.0 V for the 25-Å sample and 1.5 V for the 35-Å sample. These values were chosen to give the best match between the theoretical model discussed in Sec. IV A and the data. They are consistent with the experimentally determined voltages at which the quantum efficiency begins to drop off and the spectra show weak evidence of miniband formation. They are also similar to our previous estimates based on fitting the high field transition energies.[18] In the 25-Å sample, we observe two additional peaks approximately 25 meV below the main heavy- and light-hole transitions for $V_{appl} < +0.5$ V. We believe these additional peaks are an artifact of the sample, and are not related to the effect discussed here.[27]

In both samples, the anticrossing is best resolved for the light-hole excitons. Table I gives the estimated resonant field F_{res} and minimum line splitting δE for the

TABLE I. The estimated resonant field F_{res} and line splitting δE at the anticrossings.

Sample	Heavy holes		Light holes	
	F_{res} (kV cm^{-1})	δE (meV)	F_{res} (kV cm^{-1})	δE (meV)
25 Å	3.9	3.2	5.2	5.4
35 Å	4.1	~2.9	6.1	3.7

heavy- and light-hole transitions of the two samples. Our criterion for determining the resonant field is that the oscillator strength for the two split transitions should be equal. δE was determined directly from the spectra for the light-hole transitions, and by deconvolution for the heavy-hole transitions. We note that δE decreases as the barrier thickness increases, as expected for a tunneling process. F_{res} and δE are both slightly higher for the light holes than for the heavy holes. From Fig. 2 and the discussion in Sec. II we see that F_{res} should indeed be larger for the light holes than for heavy holes because of the larger light-hole exciton binding energy.

Our results give very clear experimental confirmation of the excitonic anticrossings predicted theoretically by Dignam and Sipe.[11,12] We are only able to observe the anticrossing between the 0 and −1 Stark-ladder states, in contrast to the family of anticrossings predicted in Refs. 11 and 12. This may be due to the fact that our interwell coupling is between the specific cases of long-period and intermediate-period superlattices considered in Ref. 12. However, it may also be an indication that the wave-function coherence is being curtailed due to imperfections in the sample. For example, Schneider *et al.* were able to observe resonant tunneling between *next*-nearest-neighbor Stark-ladder states in their GaAs/AlAs superlattice.[28] However, it should be noted that the total coherence length implied in the results of Ref. 28 is not so much greater than in our case, due to the larger superlattice period in our samples (up to 130 Å). Since we only observe the one anticrossing, we are justified in modeling the situation by considering nearest-neighbor interactions only. As discussed in Sec. II, a simple explanation of the single anticrossing can then be given if we assume that the electron-hole Coulomb interaction causes a localization of the wave functions even near $F_z = 0$. From our understanding of the physics of the 25- and 35-Å barrier samples, we would expect to be able to obtain essentially the same absorption spectra from a symmetric double-well structure with the same wells and barriers as the superlattices.

IV. THEORETICAL RESULTS

A. Variational modeling of excitons in a three-well structure

We have modeled the optical properties of the superlattice using a generalized version of our double-well variational exciton calculation.[17,18] In order to allow for nearest-neighbor interactions in the superlattice, we need to consider three quantum wells rather than the two considered previously. We thus approximated the conduction band by three coupled quantum wells, but have made the additional approximation of just considering the valence band as a single uncoupled well (see Fig. 6). The artificial constraint of the holes to be localized in just a single well was made to simplify the calculation. It is a reasonable assumption for the heavy holes in most superlattices due to the large heavy-hole effective mass. We will discuss the validity for the light holes later.

After separating off the x-y plane center-of-mass motion, the Hamiltonian is given by

$$H = H_{xy} + H_e + H_h + V_{\text{Coul}} , \tag{4}$$

where

$$H_{xy} = -\frac{\hbar^2}{2\mu_{xy}}\nabla_{xy}^2 , \tag{5}$$

$$H_e = -\frac{\hbar^2}{2m_e}\frac{\partial^2}{\partial z_e^2} + V_e(z_e) - eF_z z_e , \tag{6}$$

$$H_h = -\frac{\hbar^2}{2m_h}\frac{\partial^2}{\partial z_h^2} + V_h(z_h) + eF_z z_h , \tag{7}$$

and

$$V_{\text{Coul}} = -\frac{e^2}{4\pi\epsilon_0\epsilon}\frac{1}{\sqrt{\rho^2 + (z_e - z_h)^2}} . \tag{8}$$

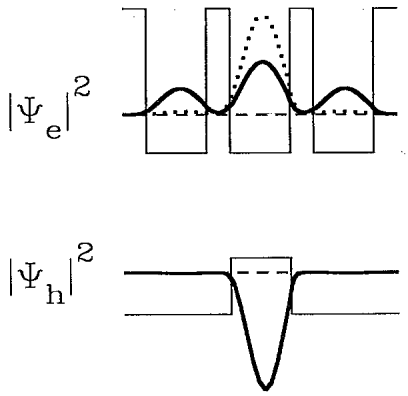

FIG. 6. Calculated electron and hole wave functions for the simplified structure used in the variational model. The results are shown for the 35-Å barrier sample at $F_z = 0$. The *single-particle* wave functions calculated without considering excitonic effects are shown by the solid lines. The dotted line shows the modified electron wave function calculated by our variational exciton model which includes the electron-hole Coulomb interaction.

The subscripts e, h refer to electrons or holes, respectively. The field F_z is assumed to be along the z direction. $V_e(z_e)$ and $V_h(z_h)$ are the potentials due to the quantum wells. m_e and m_h are the effective masses, and μ_{xy} is the reduced x-y plane electron-hole mass. ϵ is the averaged relative dielectric constant, and ρ is the x-y plane electron-hole separation, $\sqrt{x^2+y^2}$.

The exciton wave function is given by Eq. (2). The x-y plane center-of-mass motion is trivial, and we neglect it from now on. The first step to the solution is to obtain a set of basis wave functions for $\psi_e(z_e)$ and $\psi_h(z_h)$. One approach would be to solve the equations for isolated quantum wells, and then to use linear combinations of these wave functions localized in the different quantum wells in a tight-binding type of method. Instead we choose to use the single-particle wave functions of the coupled-well system with the field applied as our basis. The Coulomb interaction is then treated as a perturbation. With V_{Coul} set to zero, the equations are separable, and basis wave functions can be found by solving

$$H_e\phi_{en}(z_e) = E_{en}\phi_{en}(z_e) \tag{9}$$

and

$$H_h\phi_{hm}(z_h) = E_{hm}\phi_{hm}(z_h)\ . \tag{10}$$

This choice of basis wave functions already includes the quantum confined Stark shift of the levels, and also the simplified miniband effects of the three-well system near $F_z = 0$. As before,[17,18] we use the tunneling resonance technique to find $\phi_{hm}(z_h)$ and $\phi_{en}(z_e)$. The solid bold lines in Fig. 6 show the first electron and heavy-hole wave functions calculated at $F_z = 0$ in this way for the structures indicated.

We now consider the first three exciton states of the system. The wave function of the ith exciton is obtained by solving

$$H\Psi_i(\rho, z_e, z_h) = E_i\Psi_i(\rho, z_e, z_h)\ , \tag{11}$$

where H is now the full Hamiltonian of Eq. (4), and i runs from 1 to 3. We use a variational approach, with the following trial wave function:

$$\Psi_i^{(\text{var})}(\rho, z_e, z_h) = \varphi_{xy}^i(\rho)\,\varphi_e^i(z_e)\,\varphi_h^i(z_h)\ , \tag{12}$$

where $\varphi_{xy}^i(\rho)$, $\varphi_e^i(z_e)$, and $\varphi_h^i(z_h)$ are the variational wave functions which have to be determined for the relative x-y plane motion and the z-direction motion, respectively. For $\varphi_{xy}^i(\rho)$ we use a $1s$ wave function with variable radius $\lambda_i/2$:

$$\begin{aligned}\varphi_{xy}^i(\rho) &\equiv \phi_{1s}(\lambda_i)\\ &= \left(\frac{2}{\pi}\right)^{\frac{1}{2}}\frac{1}{\lambda_i}\exp\left(-\frac{\rho}{\lambda_i}\right)\ .\end{aligned} \tag{13}$$

To make the problem computationally easier, we make the approximation that the Coulomb interaction is weak compared to the separation of the first and second sublevels of any isolated quantum well. This means that we need only consider the three electron wave functions derived from the first sublevel of each of the three individual quantum wells. In this case, we can expand $\varphi_e^i(z_e)$ over the first three single-particle electron wave functions $\phi_{en}(z_e)$, writing

$$\varphi_e^i(z_e) = \sum_{n=1}^{3} c_{in}\phi_{en}(z_e)\ . \tag{14}$$

Here, c_{in} are variable mixing parameters to be determined. Of course, if we were to "turn off" the Coulomb interaction perturbation, the mixing coefficients would become diagonal (i.e., $c_{in} = \delta_{i,n}$), and we would revert to the Stark-ladder situation without excitonic effects. This is the limiting behavior expected at high fields, where eF_zd is much greater than the exciton binding energy. For $\varphi_h^i(z_h)$ we simply use the first Stark-shifted hole level $\phi_{h1}(z_h)$ of the central quantum well. This amounts to assuming that the barriers are thick for the heavy holes, and that the separation of the hole sublevels within the quantum well is significantly greater than the exciton binding energy.

The task of the calculation is to determine the nine mixing coefficients c_{in} and the three exciton radii $\lambda_i/2$ as a function of F_z. With the three normalization and three mutual orthogonality constraints on Ψ_i, this amounts to six independent parameters. We determine these parameters variationally. The first three of the variational parameters are obtained by minimizing the energy of the ground-state exciton. Our approach is to vary the mixing coefficients first and then vary the radii. Thus we first find the minimum energy corresponding to a particular value of λ. This is the lowest eigenvalue $E_{\min}(\lambda)$ of the $[3\times 3]$ Hamiltonian matrix $\mathbf{H}(\lambda)$, where the individual matrix elements $H_{nn'}(\lambda)$ are given by

$$\begin{aligned}H_{nn'}(\lambda) &\equiv \langle\phi_{en}\phi_{h1}\phi_{1s}(\lambda)|H|\phi_{en'}\phi_{h1}\phi_{1s}(\lambda)\rangle\\ &= \delta_{n,n'}\left(E_{en}+E_{h1}+\frac{\hbar^2}{2\mu\lambda^2}\right)\\ &\quad+\langle\phi_{en}\phi_{h1}\phi_{1s}(\lambda)|V_{\text{Coul}}|\phi_{en'}\phi_{h1}\phi_{1s}(\lambda)\rangle\ .\end{aligned} \tag{15}$$

The evaluation of the Coulomb integral is discussed in Refs. 7 and 18. Having found $E_{\min}(\lambda)$, we then vary λ itself to obtain the true minimum energy subject to our choice of the variational wave function set out in Eqs. (12)–(14). Let the value of λ which minimizes $E_{\min}(\lambda)$ be called $\lambda_{\min}$. Then by the variational principle, $E_{\min}(\lambda_{\min})$ is the best estimate for the energy of the ground-state exciton E_1, and $\lambda_{\min}$ is the best estimate for the exciton diameter, λ_1. The eigenvector of $\mathbf{H}(\lambda_1)$ corresponding to E_1 gives best estimate for the mixing coefficients c_{11}, c_{12}, and c_{13}. Because of the normalization constraint, this amounts to determining just two of the three unknown mixing coefficients.

To find the next two variational parameters, we minimize the energy of the first excited state subject to the constraint that its wave function must be orthogonal to the ground state. This latter constraint is conveniently satisfied if we choose the wave function to be a linear combination of the two other eigenvector wave functions of $\mathbf{H}(\lambda_1)$, which we call $\Phi_2(z_e)$ and $\Phi_3(z_e)$. This implies that we use the following variational wave function for

the first excited state:

$$\Psi_2^{(\mathrm{var})}(\lambda,\theta) = (\cos\theta\,\Phi_2 - \sin\theta\,\Phi_3)\phi_{1h}\,\phi_{1s}(\lambda)\ , \quad (16)$$

where λ and θ are the variational parameters to be determined. θ is introduced for convenience since $\sin^2\theta + \cos^2\theta = 1$; it has no particular physical significance. We minimize the energy by first varying θ to get the minimum energy for a particular value of λ, and then we vary λ itself. We call the values of θ and λ which minimize the energy $\theta_{\min}$ and $\lambda'_{\min}$. By the variational principle, these are the best approximations for the first excited state. Hence we obtain the best estimates for the energy E_2, diameter λ_2, and wave function Ψ_2 of the first excited state.

There remains one last variational parameter to determine: the diameter λ_3 of the second excited state exciton. The constraint of orthogonality has fully determined the z_e part of its wave function to be $(\sin\theta_{\min}\,\Phi_2 + \cos\theta_{\min}\,\Phi_3)$. Thus we have to minimize the energy by varying just the exciton radius, and thereby obtain the best estimate for E_3 and λ_3.

The results of the calculation for the 25- and 35-Å barrier samples are shown superimposed over the experimental data points in Figs. 4(b) and 5(b). The dotted lines are for the heavy-hole transitions and the dashed lines for the light holes. The +1 Stark-ladder transition energy is not shown because the calculated electron-hole overlap is negligibly small. This reduced oscillator strength of the +1 transition has been discussed previously by Whittaker.[14] The parameters used for the fits were the same as before[17,18] to within 2% . We used a value of 0.0512 for the in-plane light-hole reduced mass. Our model is seen to give excellent agreement with the experimental data. The wave function shown by the dotted line in Fig. 6 is the z_e part of Ψ_1 at $F_z = 0$ for the 35-Å barrier sample. The localizing effect of the electron-hole Coulomb interaction on the electron wave function is very evident in this case.

B. Full exciton calculation

In addition to the variational method just discussed, we present here an exciton Green's-function[29] approach from which we can calculate not only the energies of the exciton peaks but also the entire photocurrent spectra. We start with writing the exciton wave function as

$$\Psi_i(\rho, z_e, z_h) = \sum_{nm} \psi^i_{nm}(\rho)\phi_{en}(z_e)\phi_{hm}(z_h) \quad (17)$$

and solve the unknown function $\psi^i_{nm}(\rho)$ directly, instead of variationally. Performing a two-dimensional (2D) Fourier transform, we can change the original exciton effective-mass equation in coordinate space into an integral equation in k space,

$$\left(E_{en} + E_{hm} + \frac{\hbar^2 k^2}{2\mu_{xy}}\right)\Phi^i_{nm}(k) + \sum_{n'm'}\int \frac{d^2\mathbf{k}'}{(2\pi)^2} V_{nmn'm'}(\mathbf{k}-\mathbf{k}')\Phi^i_{n'm'}(k') = E_i\Phi^i_{nm}(k)\ , \quad (18)$$

where

$$V_{nmn'm'}(\mathbf{q}) = \frac{-e^2}{2\epsilon_0\epsilon q}\int dz_e \int dz_h \phi_{en}(z_e)\phi_{en'}(z_e)\phi_{hm}(z_h)\phi_{hm'}(z_h)e^{-q|z_e - z_h|}\ ,$$

$$\psi^i_{nm}(\rho) = \int \frac{d^2\mathbf{k}}{(2\pi)^2}\Phi^i_{nm}(k)e^{i\mathbf{k}\cdot\rho}\ .$$

Replacing $\int d^2\mathbf{k}$ by $\int_0^{2\pi} d\phi \int_0^\infty k dk$ and mapping the semi-infinite interval $(0,\infty)$ to a finite interval by a change of variable, the above equation is then solved numerically using a modified Gaussian quadrature method. Details of taking care of the singularity of the potential $V_{nmn'm'}(q)$ at $q = 0$ are described in Ref. 29 and not repeated here. The advantage of this formulation is that the exciton excited states and the continuum states are included automatically and treated on an equal footing with the ground state.

After solving Eq. (18), we then calculate the absorption coefficient α using the same method as that in Ref. 29. Finally, the photocurrent is obtained by $I = I_0(1 - e^{-\alpha L})$. There are no adjustable parameters in the calculation except that the linewidths, 4.5 meV for the heavy hole and 5 meV for the light hole, are chosen to mimic the experimental data. We also find that a Gaussian line shape fits the data better than a Lorentzian. For the 25- and 35-Å samples, we use a two-well model and include the two lowest conduction subbands (i.e., the two n=1 coupled subbands) and the two lowest valence subbands for both the heavy and light holes. The results are shown in Figs. 7(a) and 7(b). The peak positions of the photocurrent spectra, the field dependence, and the energy splittings agree very well with the experimental data. Although a quantitative match between the absolute magnitude and the data is still lacking, the overall features of the spectra are clearly shown. Therefore, we may conclude that the observed anticrossings between the intrawell and interwell excitons in the 25- and 35-Å samples are well understood with the two-well model. On the other hand, for the 15-Å sample, we find that even a full three-coupled-well calculation, including three conduction subbands and three valence subbands, is not adequate to account for the data. This is in fact expected because the tendency toward miniband formation and wave-function delocalization is much stronger in the 15-Å sample than that in the 25- and 35-Å samples.

C. Discussion

We have presented two different theoretical approaches to the exciton states of our superlattices in an electric field, both of which are essentially coupled well rather than superlattice models. We have shown that we obtain excellent agreement with the experimental data. The physical reason why these coupled-well models work so well is that the excitonic effects are collapsing the delocalized superlattice wave functions into localized states. For example, Fig. 6 illustrates the case where the presence of a localized heavy hole causes the electron wave function also to be localized mostly in the well where the hole is localized. At finite field, the next electron level is localized in a different well from the hole, and so we do not observe a Stark ladder because the oscillator strength of the interwell transitions is too small.

It is clear that the variational model of Sec. IV A should not work for the light holes, because the calculated light-hole miniband width is comparable to or even greater than that of the electrons. This means that the artificial constraint of having localized hole levels is totally unrealistic in this case. On the other hand, the calculations fit the experimental data very well. One possible explanation as to why the model works so well can be made by comparing our approach to that of Chomette *et al.*, who made variational calculations of the exciton states of a superlattice at zero applied field.[30] On varying the localization parameter β in their calculation, they found two minima in the energy corresponding to situations in which the wave function is delocalized over several wells or is essentially totally localized in just one well. The delocalized minimum had the lower energy for $d \lesssim 94$ Å, whereas for $d \gtrsim 94$ Å the localized minimum had the lower energy. Our three superlattices have a period d close to the transition value, although in our case, d is not a particularly useful parameter due to the large imbalance between the well and barrier thicknesses. We speculate that if we were to perform a similar calculation to that shown in Fig. 3 of Ref. 30 for the case of a fixed 95-Å well width but variable barrier width, we would find that the transition between delocalized and localized behavior would occur between L_b=15 and 25 Å. By choosing a localized hole wave function at the outset, our calculation cannot find the minimum in energy corresponding to delocalized wave functions, but we find empirically that this does not matter. Physically, what is happening is that the Coulomb interaction is pulling the electron and hole wave functions close together. In the case of the light holes, the criterion we gave, namely $\Delta E/2 \lesssim E_x$, has to be modified to include the *sum* of both electron and hole miniband widths in ΔE. Note that the full two-well exciton calculation of Sec. IV B allows for mixing of hole bands as well as electron bands, and the same anticrossing behavior is predicted.

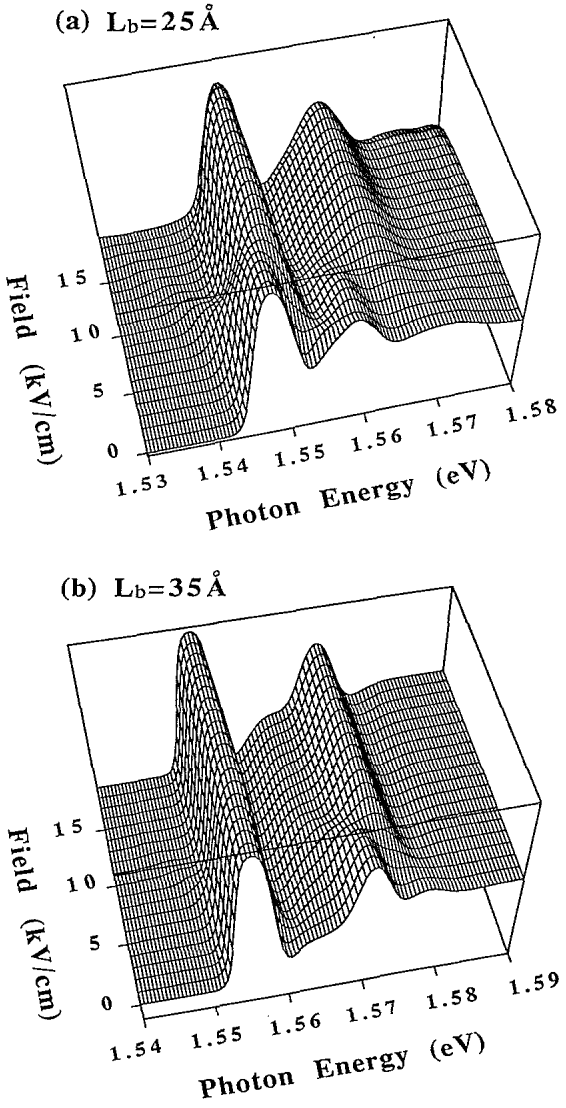

FIG. 7. Theoretical photocurrent spectra against bias field for a two-coupled-well model. The barrier widths are (a) 25 Å and (b) 35 Å.

It is interesting to conjecture whether these excitonic localization effects may be partly responsible for the unusually strong oscillator strength observed in shallow quantum-well superlattices.[31] In that situation the superlattice miniband widths are also comparable to typical exciton binding energies, and so the effects we discuss here should be important. It is also interesting to relate our results to the recently reported observation of Bloch oscillations in a semiconductor superlattice by Feldmann *et al.*[32] The sample used in Ref. 32 was in fact the same as the 15-Å barrier sample studied here. We see that the reason why they were successful was that the sample satisfies the criterion $\Delta E/2 > E_x$. Had they used a sample with a smaller miniband width, the excitonic effects would probably have prevented the observation of the Bloch oscillations.

V. CONCLUSIONS

In conclusion, we have studied how excitonic effects localize the wave functions in superlattices with miniband widths of ~10 meV or less. This localization drastically alters the behavior of the optical spectra in the Stark-ladder regime: we observe a single excitonic an-

ticrossing as observed previously in coupled double-well structures rather than the superlattice Stark-ladder fan diagram. We have been able to explain this anticrossing using a coupled double-well model rather than a superlattice model. The implication of this work is that the conceptual distinction between a "superlattice" and a "multiple-quantum-well" structure is affected by excitonic effects. In principle, all periodic quantum-well structures are "superlattices." In practice, however, the distinction made between localized quantum-well behavior and delocalized superlattice behavior is a useful one. The usual criterion which determines the two types of behavior is the thickness of the barriers separating the quantum wells. We have shown that there is an additional factor which must be considered in an optical experiment, namely the ratio of half the miniband width to the quantum-well exciton binding energy.

ACKNOWLEDGMENTS

The work at the University of Illinois was supported by the Office of Naval Research under Grant No. N00014-90-J-1821, the Joint Service Electronics Program under Grant No. N00014-90-J-1270, and the National Center for Supercomputing Applications at the University of Illinois. We acknowledge helpful discussions with A.J. Turberfield, and would like to thank J.E. Henry and M.M. Becker at AT&T for the processing of the samples.

[1]See, for example, G. H. Wannier, *Elements of Solid State Theory* (Cambridge University Press, Cambridge, England, 1959), pp. 190–193.
[2]L. Esaki and R. Tsu, IBM J. Res. Dev. **14**, 61 (1970).
[3]E. E. Mendez, G. Bastard, L. L. Chang, L. Esaki, H. Morkoç, and R. Fischer, Phys. Rev. B **26**, 7101 (1982).
[4]R. C. Miller and A. C. Gossard, Appl. Phys. Lett. **43**, 954 (1983).
[5]T. H. Wood, C. A. Burrus, D. A. B. Miller, D. S. Chemla, T. C. Damen, A. C. Gossard, and W. Wiegmann, Appl. Phys. Lett. **44**, 16 (1984).
[6]D. A. B. Miller, D. S. Chemla, T. C. Damen, A. C. Gossard, W. Wiegmann, T. H. Wood, and C. A. Burrus, Phys. Rev. Lett. **53**, 2173 (1984).
[7]D. A. B. Miller, D. S. Chemla, T. C. Damen, A. C. Gossard, W. Wiegmann, T. H. Wood, and C. A. Burrus, Phys. Rev. B **32**, 1043 (1985).
[8]J. Bleuse, G. Bastard, and P. Voisin, Phys. Rev. Lett. **60**, 220 (1988).
[9]E. E. Mendez, F. Agullo-Rueda, and J. M. Hong, Phys. Rev. Lett. **60**, 2426 (1988).
[10]R. H. Yan, F. Laruelle, and L. A. Coldren, Appl. Phys. Lett. **55**, 2002 (1989).
[11]M. M. Dignam and J. E. Sipe, Phys. Rev. Lett. **64**, 1797 (1990).
[12]M. M. Dignam and J. E. Sipe, Phys. Rev. B **43**, 4097 (1991).
[13]D. M. Whittaker, Phys. Rev. B **41**, 3238 (1990).
[14]D. M. Whittaker, Superlatt. Microstruct. **7**, 375 (1990).
[15]R. P. Leavitt and J. W. Little, Phys. Rev. B **42**, 11 784 (1990).
[16]N. F. Johnson, J. Phys. Condens. Matter **2**, 2099 (1990).
[17]A. M. Fox, D. A. B. Miller, G. Livescu, J. E. Cunningham, J. E. Henry, and W. Y. Jan, Phys. Rev. B **42**, 1841 (1990).
[18]A. M. Fox, D. A. B. Miller, G. Livescu, J. E. Cunningham, and W. Y. Jan, Phys. Rev. B **44**, 6231 (1991).
[19]E. E. Mendez, F. Agullo-Rueda, and J. M. Hong, Appl. Phys. Lett. **56**, 2545 (1990).
[20]M. F. Pereira, Jr., I. Galbraith, S. W. Koch, and G. Duggan, Phys. Rev. B **42**, 7084 (1990).
[21]See, for example, G. Bastard, *Wave Mechanics Applied to Semiconductor Heterostructures* (Wiley, New York, 1988).
[22]I. Galbraith and G. Duggan, Phys. Rev. B **40**, 5515 (1989).
[23]R. Ferreira, C. Delalande, H. W. Liu, G. Bastard, B. Etienne, and J. F. Palmier, Phys. Rev. B **42**, 9170 (1990).
[24]R. P. Leavitt and J. W. Little, Phys. Rev. B **42**, 11 774 (1990).
[25]A. M. Fox, D. A. B. Miller, G. Livescu, J. E. Cunningham, and W. Y. Jan, IEEE J. Quantum Electron. **27**, 2281 (1991).
[26]The fact that we observe an anticrossing for both heavy- and light-hole transitions suggests the possibility that we are observing resonant tunneling between light- and heavy-hole states [C. Y.-P. Chao and S. L. Chuang, Phys. Rev. B **43**, 7027 (1991)]. This would be possible because the average $k_{\|}$ of an exciton is $\sim 10^6$ cm^{-1}, which implies substantial intermixing of the heavy- and light-hole bands [Altarelli *et al.*, Phys. Rev. B **32**, 5138 (1985)]. Resonant tunneling between the first heavy- and light-hole bands of adjacent wells is expected to occur at resonant fields $F_{\rm res} \sim 9$ kV cm^{-1}, fairly close to that observed experimentally. Close inspection of the experimental data, however, makes this explanation implausible. Our main reason for discounting heavy-hole–light-hole resonant tunneling is based on an experimental inconsistency. If the heavy and light holes were anticrossing with each other, we would expect to be able to observe two transitions associated with either the heavy-hole exciton transitions or the light-hole transitions, as indeed is the case observed experimentally at fields close to resonance. However, the behavior expected for the light and heavy holes is different. The weaker transition of the heavy-hole doublet would be expected to be on the higher-energy side of the main peak for $F < F_{\rm res}$ and at lower energy for $F > F_{\rm res}$. By contrast, the weaker transition for the light-hole doublet should be at *lower* energy to the main light-hole peak below $F_{\rm res}$ and at *higher* energy above $F_{\rm res}$. Experimentally, we observe that below $F_{\rm res}$ the weaker transition is at higher energy for *both* the heavy-hole and light-hole transitions. Similarly, above $F_{\rm res}$ the weaker transition is at lower energy for both types of transition. Thus although heavy-hole–light-hole resonant tunneling might be occurring, it is clearly not the dominant effect.
[27]The origin of these peaks is not fully determined at present. The most likely explanation is that a few extra layers were accidentally included in the structure during growth. Another possible explanation is suggested by the fact that they lie $\sim$ 25 meV below the main transitions, which points to bound excitons at beryllium acceptors. It is possible that the beryllium p-type dopant may have diffused into a few of the wells near the p-type layer. The three samples were grown in different batches, so that it is reasonable that acceptor lines should be seen in one of the samples but not the others. This explanation is less probable than the first be-

cause bound excitons are not usually observed in aborption-related spectra. In both cases the apparent strength of weak absorption lines relative to strong lines is exaggerated in photocurrent spectra, where the signal is proportional to $(1 - e^{-\alpha L})$ rather than α itself, α being the absorption coefficient. Hence these additional peaks are in fact much weaker compared to the main heavy- and light-hole transitions than they appear in the spectra. We do not think they are related to the effects discussed here because the anti-crossings are observed in both the 25- and 35-Å samples, whereas the peaks are only observed in the 25-Å sample.

[28]H. Schneider, H. T. Grahn, K. v. Klitzing, and K. Ploog, Phys. Rev. Lett. **65**, 2720 (1990).

[29]S. L. Chuang, S. Schmitt-Rink, D. A. B. Miller, and D. S. Chemla, Phys. Rev. B **43**, 1500 (1991).

[30]A. Chomette, B. Lambert, B. Deveaud, F. Clerot, A. Regreny, and G. Bastard, Europhys. Lett. **4**, 461 (1987).

[31]K. W. Goossen, J. E. Cunningham, and W. Y. Jan, Appl. Phys. Lett. **57**, 2582 (1990).

[32]J. Feldmann, K. Leo, J. Shah, D. A. B. Miller, J. E. Cunningham, S. Schmitt-Rink, T. Meier, G. von Plessen, A. Schulze, and P. Thomas, Phys. Rev. B **46**, 7252 (1992).